

A New Computationally Efficient Measure of Topological Redundancy of Biological and Social Networks

Réka Albert*

Department of Physics, Pennsylvania State University, University Park, PA 16802

Bhaskar DasGupta,[†] Rashmi Hegde,[‡] and Gowri Sangeetha Sivanathan[§]
Department of Computer Science, University of Illinois at Chicago, Chicago, IL 60607

Anthony Gitter[¶]

Computer Science Department, Carnegie Mellon University, Pittsburgh, PA

Gamze Gürsoy**

Department of Bioengineering, University of Illinois at Chicago, Chicago, IL 60607

Pradyut Paul^{††}

Junior, Neuqua Valley High School, Naperville, IL 60564

Eduardo Sontag^{‡‡}

Department of Mathematics, Rutgers University, New Brunswick, NJ 08903

(Dated: July 14, 2024)

It is well-known that biological and social interaction networks have a varying degree of redundancy, though a consensus of the precise cause of this is so far lacking. In this paper, we introduce a topological redundancy measure for labeled directed networks that is formal, computationally efficient and applicable to a variety of directed networks such as cellular signaling, metabolic and social interaction networks. We demonstrate the computational efficiency of our measure by computing its value and statistical significance on a number of biological and social networks with up to several thousands of nodes and edges. Our results suggest a number of interesting observations: **(1)** social networks are more redundant than their biological counterparts, **(2)** transcriptional networks are less redundant than signaling networks, **(3)** the topological redundancy of the *C. elegans* metabolic network is largely due to its inclusion of currency metabolites, and **(4)** the redundancy of signaling networks is highly (negatively) correlated with the monotonicity of their dynamics.

PACS numbers: 87.18.Mp, 87.18.Vf, 89.75.Hc, 87.85.Xd

Keywords: Networks, Redundancy, Dynamics

I. INTRODUCTION

The concepts of degeneracy and redundancy are well known in information theory. Loosely speaking, *degeneracy* refers to structurally different elements performing the same function, whereas *redundancy* refers to identical elements performing the same function¹. In electronic systems, such measures are useful in analyzing properties

such as fault-tolerance. It is an accepted fact that biological networks do *not* necessarily have the lowest possible degeneracy or redundancy; for example, the connectivity of neurons in brains suggest a high degree of degeneracy [2]. However, as Tononi, Sporns and Edelman observed in their paper [3]:

Although many similar examples exist in all fields and levels of biology, a specific notion of degeneracy has yet to be firmly incorporated into biological thinking, largely because of the lack of a formal theoretical framework.

The same comment holds true about redundancy as well. A further reason for the lack of incorporation of these notions in biological thinking is the lack of *effective* algorithmic procedures for computing these measures for large-scale networks even when formal definitions are available.

* ralbert@phys.psu.edu; www.phys.psu.edu/~ralbert

† dasgupta@cs.uic.edu; www.cs.uic.edu/~dasgupta; Author to whom correspondence should be sent.

‡ rashmihegde.g@gmail.com

§ gsivan2@uic.edu

¶ agitter@cs.cmu.edu; www.cs.cmu.edu/~agitter

** gamze.gursoy@gmail.com; www2.uic.edu/~ggurso2

†† paulpradyut@yahoo.com

‡‡ sontag@math.rutgers.edu; www.math.rutgers.edu/~sontag

¹ We remind the reader that the term “redundancy” is *also* used in other contexts in biology unrelated to the definition of redundancy in this paper. For example, some researchers use redundancy to refer to *paralogous genes* that can provide *functional backup* for one another [1]. In addition, some researchers use the

two terms, redundancy and degeneracy, interchangeably or use other terminologies for these concepts.

Therefore, such studies are often done in a somewhat ad-hoc fashion, as in [4]. There do exist notions of “redundancy” in the field of analysis of *undirected* networks based on clustering coefficients (*e.g.*, see [5]) or betweenness centrality measures (*e.g.*, see [6]). However, such notions are not appropriate for the analysis of biological networks where one must distinguish positive from negative regulatory interactions, and where the study of dynamics is of interest.

II. BRIEF REVIEW OF AN INFORMATION-THEORETIC DEGENERACY AND REDUNDANCY MEASURES

Formal information-theoretic definitions of degeneracy and redundancy for dynamic biological systems were proposed in [3] (see also [7, 8]) based on *mutual-information contents*. These definitions assume access to suitable perturbation experiments and corresponding accurate measurements of the relevant parameters. Thus, they are *not* directly comparable to the topology-based redundancy measures that we propose in this paper. Nonetheless, we next briefly review these definitions as a way to illustrate some key points of other measures often used in the literature that motivated us to define our new redundancy measure.

The authors of [3] consider system consisting of n elements that produces a set of outputs \mathcal{O} via a fixed connectivity matrix from a subset of these elements. The elements are described by a jointly distributed random vector X that represents steady-state activities of the components of their system. The degeneracy $\mathcal{D}(X; \mathcal{O})$ of the system is then expressed as the average mutual information (MI) shared between \mathcal{O} and the “perturbed” bi-partitions of X summed over all bipartition sizes (Equation [2b] of [3]), *i.e.*,

$$\mathcal{D}(X; \mathcal{O}) = \frac{1}{2} \times \sum_{k=1}^n \sum_j \left(\text{MI}^P(X_j^k; \mathcal{O}) + \text{MI}^P(X \setminus X_j^k; \mathcal{O}) - \text{MI}^P(X; \mathcal{O}) \right) \quad (1)$$

where X_j^k is a j^{th} subset of X composed of k elements and the notation $\text{MI}^P(\mathcal{A}; \mathcal{O})$ denotes the mutual information between a subset of elements \mathcal{A} and an output set \mathcal{O} , when \mathcal{A} is injected with a small fixed amount of uncorrelated noise²; see [3, 7] for details. One can immediately see a computational difficulty in applying such a definition: *the number of possible bipartitions could be astronomically large even for a modest size network*. For

example, for a network with 100 nodes which is a number smaller than all but one of the networks considered in this paper, the number of bi-partitions is roughly $2^{100} > 10^{30}$. Measures avoiding averaging over all bi-partitions were also proposed in [3], but the computational complexities and accuracies of these measures remain to be thoroughly investigated and evaluated on larger networks.

In a similar manner, the redundancy $\text{R}(X; \mathcal{O})$ of a system X was defined in [3] as the difference between summed mutual information upon perturbation between all subsets of size up to 1 and \mathcal{O} , and the mutual information between the entire system and \mathcal{O} (Equation [3] in [3]), *i.e.*,

$$\text{R}(X; \mathcal{O}) = \sum_{j=1}^n \text{MI}^P(X_j^1; \mathcal{O}) - \text{MI}^P(X; \mathcal{O}) \quad (2)$$

Note that a clear shortcoming of this measure is that it only provides a number, but does not indicate which subset of elements are redundant. Identifying redundant elements is important for the interpretation of results, and may also serve as an important step of the network construction and refinement process, as we will illustrate in our application to the *C. elegans* metabolic network and the oriented PPI network. Tononi, Sporns and Edelman [3] illustrated the above measure on a few model networks as a proof of concept, but large networks clearly necessitate alternate measures that allow *efficient* calculations.

In this paper we propose a new *topological* measure of redundancy. A benefit of our new redundancy measure is that we can *actually find an approximately minimal network* and, in the case of multiple minimal networks of similar quality, a subset of them by enabling a randomization step in the algorithmic procedure. We determine this redundancy value for a number of biological and social networks of large sizes and observe a number of interesting properties of our redundancy measure.

III. MODELS FOR DIRECTED BIOLOGICAL AND SOCIAL NETWORKS

There are two very different levels of models for biological systems. A so-called *network topology* model (also known as a “wiring diagram” or a “static graph”) provides a coarse diagram or map of the physical, chemical, or statistical connections between molecular components of the network, without specifying the detailed kinetics. In this type of model, a network of molecular interactions is viewed as a graph: cellular components are nodes in a network, and the interactions between these components are represented by edges connecting the nodes. In this paper, we are mainly concerned with this type of model; exact details are described in Section III A.

In the other type of model, a *network dynamics* model, mathematical rules (*e.g.*, systems of Boolean rules or differential equations) are used to specify the behavior over

² $\text{MI}^P(\mathcal{A}; \mathcal{O}) = \mathcal{H}(\mathcal{A}) + \mathcal{H}(\mathcal{O}) - \mathcal{H}(\mathcal{A}, \mathcal{O})$, where $\mathcal{H}(\mathcal{A})$ and $\mathcal{H}(\mathcal{O})$ are the entropies of \mathcal{A} and \mathcal{O} considered independently, and $\mathcal{H}(\mathcal{A}, \mathcal{O})$ is the joint entropy of the subset of elements \mathcal{A} and the output set \mathcal{O} .

time of each of the molecular components in the network. Our investigation is not directly concerned with such dynamic models. However, since we will show a correlation of our redundancy measure for the network topology model with a property, namely *monotonicity*, of an associated network dynamics model, we briefly review this model in Section III B.

A. Network Topology Model

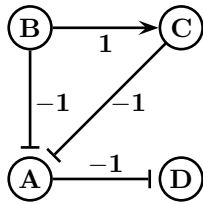


FIG. 1. The network topology model for biological networks. The parity of the pathway $B \rightarrow C \rightarrow A \rightarrow D$ is $1 \times (-1) \times (-1) = 1$.

Three common types of molecular biological networks are: *transcriptional regulatory* networks, *metabolic* networks, and *signaling* networks. The nodes of transcriptional regulatory networks represent *genes*, and edges represent (positive or negative) regulation of a given gene’s *expression* by proteins associated to other genes. The nodes of metabolic networks are metabolites and the edges represent the *enzyme-catalyzed* reactions in which these metabolites participate as reactants or products. The nodes of signaling networks are proteins and small molecules, and the edges represent physical or chemical interactions or indirect positive or negative causal effects. A unified formalism to describe all these types of networks uses a *directed* graph $G = (V, E, w)$ with vertex set V , edge set E , and an edge labeling function $w : E \mapsto \{-1, +1\}$ in which a label of 1 (respectively, -1) represents an positive (respectively, negative) influence. A pathway is then a path P from vertex u to vertex v , and the excitory or inhibitory nature of the pathway is specified by the *parity* $\prod_{e \in P} w(e) \in \{-1, +1\}$ of such a path P ; see Fig. 1 for an illustration.

Our model for directed social interaction networks is simply a directed graph in which edges represent significant relationships between the entities, *e.g.*, nodes may represent web-pages and directed edges may represent hyper-links of one web-page in another. Obviously, we can think of such a model as one of the above type in which all edges are labeled $+1$ (and, thus all paths have the same parity); this allows us to treat both social and biological networks in a mathematically uniform manner for the purpose of designing and analyzing algorithms.

B. Network Dynamics and Monotonicity

Consider systems modeled via ordinary differential equations:

$$\frac{dx_i(t)}{dt} = f_i(x_1(t), x_2(t), \dots, x_n(t)) \quad \text{for } i=1, 2, \dots, n \quad (3)$$

where $x_i(t)$ indicates the concentration of the i^{th} entity in the model at time t and the f_i ’s are functions of n variables. We assume that $x(t) = (x_1(t), x_2(t), \dots, x_n(t))$ evolves in an open subset of \mathbb{R}^n , the f_i ’s are differentiable, and solutions are defined for $t \geq 0$. For example, a simple two species interaction could be described by

$$\frac{dx_1}{dt}(t) = 3x_1(t) - 5x_2(t)$$

$$\frac{dx_2}{dt}(t) = x_1(t) + x_2(t).$$

A particularly appealing class of dynamics is that of *monotone* systems [9, 10]. Informally, the dynamics of a monotone system preserves a specific partial order (hierarchy) of its inputs over time. Mathematically, monotonicity can be defined as follows.

Definition 1 [9, 10] *Given a partial order \preceq over \mathbb{R}^n , system (3) is said to be monotone with respect to \preceq if*

$$\begin{aligned} \forall t \geq 0: (x_1(0), \dots, x_n(0)) \preceq (y_1(0), \dots, y_n(0)) \\ \implies (x_1(t), \dots, x_n(t)) \preceq (y_1(t), \dots, y_n(t)) \end{aligned}$$

where $(x_1(t), \dots, x_n(t))$ and $(y_1(t), \dots, y_n(t))$ are the solutions of (3) with initial conditions $(x_1(0), \dots, x_n(0))$ and $(y_1(0), \dots, y_n(0))$, respectively.

We will restrict our attention to *orthant* orders. These are the partial orders \preceq_s over \mathbb{R}^n , for any given $s = (s_1, \dots, s_n) \in \{-1, 1\}^n$, defined as (see [10–12]):

$$x \preceq_s y \iff \forall i: s_i x_i \leq s_i y_i$$

In particular, the “cooperative order” is the partial order \preceq_s for $s = (1, 1, \dots, 1)$.

Monotone systems constitute a nicely behaved class of dynamical systems in several ways. For example, for these systems pathological behaviors (chaotic attractors) are ruled out. Even though they may have an arbitrarily large dimensionality, monotone systems (under an additional irreducibility assumption) behave in many ways like one-dimensional systems; for example, bounded trajectories generically converge to steady states, and stable oscillatory behaviors do not exist. Monotonicity with respect to orthant orders is equivalent to the non-existence of negative loops in systems; analyzing the behaviors of such loops is a long-standing topic in biology in the context of regulation, metabolism and development, starting from the work of Monod and Jacob in 1961 [13]. In this paper, we will define a measure of “degree of monotonicity” for dynamical systems and relate it to our topology-based redundancy measure.

IV. A NEW MEASURE OF REDUNDANCY

We will use the following notations for conciseness:

- For any two vertices u and v , $u \xrightarrow{x} v$ (respectively, $u \xrightarrow{-x} v$) denotes a *path* (respectively, an *edge*) from u to v of parity x . We include the empty path $u \xrightarrow{1} u$ for each vertex u .
- For any $E' \subseteq E$, $\text{reachable}(E')$ is the set of all *ordered* triples (u, v, x) such that $u \xrightarrow{x} v$ exists in the subgraph (V, E') .

For example, for the network in Fig. 1, $B \xrightarrow{1} D$ exists because of the path $B \dashv A \dashv D$ and also because of the path $B \rightarrow C \dashv A \dashv D$, and $\text{reachable}(\{B \rightarrow C, A \dashv D\}) = \{(A, A, 1), (B, B, 1), (C, C, 1), (D, D, 1), (B, C, 1), (A, D, -1)\}$.

We next state a combinatorial optimization problem that will be needed in order to introduce our new redundancy measure.

Problem name:: Binary Transitive Reduction (BTR).

Instance:: a directed graph $G = (V, E)$ with a subset of edges $E_{\text{fixed}} \subset E$ and an edge labeling function $w : E \mapsto \{-1, 1\}$.

Valid Solution:: a subgraph $G' = (V, E')$ such that

- $E' \supseteq E_{\text{fixed}}$ and
- $\text{reachable}(E') = \text{reachable}(E)$.

($E \setminus E'$ is referred to as a set of “redundant” edges.)

Goal:: minimize $|E'|$.

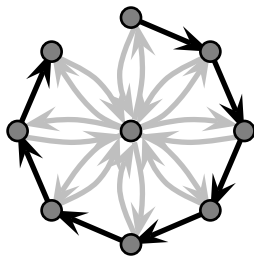


FIG. 2. Choosing one wrong edge may cost too much in BTR.

Intuitively, the BTR problem prunes pathways for which alternate equivalent pathways exist (*e.g.*, see [14, 15]). The set of edges in E_{fixed} in the definition of BTR represents edges that may *not* be removed during the algorithm; this is useful in the context when one wishes to reduce a network while preserving specific pathways.

For the redundancy calculations performed in this paper, we assume no prior knowledge of direct interactions; thus for the rest of the paper we set $E_{\text{fixed}} = \emptyset$. As an illustration, in Fig. 1 if we let $E' = E \setminus \{B \dashv A\}$ then $\text{reachable}(E') = \text{reachable}(E)$ because of the path $B \rightarrow C \dashv A$.

Finding a maximum set of edges that can be removed is non-trivial; in fact, the problem is NP-hard [16]. To illustrate the algorithmic difficulties, consider the network shown in Fig. 2. Removal of all the black edges provides a non-optimal solution of BTR, whereas an optimal solution with about half the edges compared to the non-optimal solution can be obtained by keeping all the black edges and removing all but two of the gray edges. The special case of BTR with $E_{\text{fixed}} = \emptyset$ and $w(e) = 1$ for all edges e is the so-called classical *minimum equivalent digraph* problem, and it has been investigated extensively in the context of checking minimality of connectivity requirements in computer networks (*e.g.*, see [16]). Other examples of applications of BTR-type network optimizations include the work by Wagner [17] employing a special case of BTR to determine network structure from gene perturbation data in the context of biological networks and the work by Dubois and Cécile [18] in the context of social network analysis and visualization.

Based on the BTR problem, we propose a new *combinatorial* measure of redundancy that can be computed efficiently. Note that BTR does not change pathway level information of the network and removes edges from one node to another only when a similar alternate pathway exists, thus truly removing redundant connections. Thus, $\frac{|E'|}{|E|}$ provides a measure of global compressibility of the network and our proposed new redundancy measure R_{new} is defined to be

$$R_{\text{new}} = 1 - \frac{|E'|}{|E|} \quad (4)$$

The $|E|$ term in the denominator of the above definition translates to a “min-max normalization” of the measure [19], and ensures that $0 < R_{\text{new}} < 1$. Note that *the higher the value of R_{new} is, the more redundant the network is.*

A. Properties of Our Topological Redundancy Measure and Applications of a Minimal Network

Any topological redundancy measure should have a desirable property: *the measure must not only reflect simple connectivity properties such as degree-sequence or average degree, it must also depend on higher-order connectivity.* Our redundancy measure indeed has this property, since paths of *arbitrary* length are considered for removal of an edge. For a concrete example, consider two graphs shown in Fig. 3; the in-degree and out-degree sequence of each graph is $1, 1, \dots, 1, 1, 2, 2, \dots, 2$, but their redundancy values are drastically different. Similarly, higher

average degree does not necessarily imply higher values of redundancy; for example, the network in Fig. 3, when generalized on n nodes, has an average degree below 2 and a redundancy value of roughly 0.33, whereas the graph $K_{\frac{n}{2}, \frac{n}{2}}$ (a completed bipartite graph with each partition having $n/2$ nodes and all edges directed from the left to the right partition) has an average degree of $n/2$ but a redundancy value of 0.

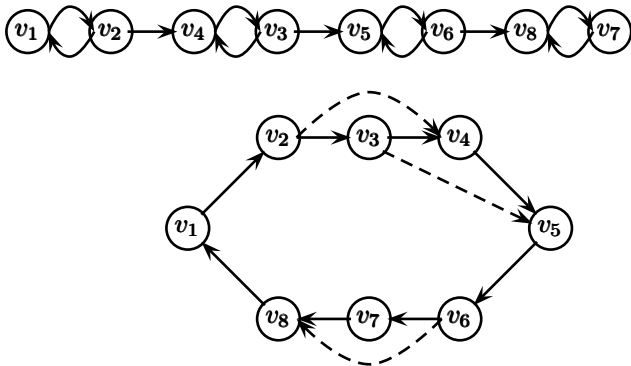


FIG. 3. Two n -node graphs with same degree sequence but with different values of R_{new} , shown for $n = 8$. The top graph has no redundant edges, thus for it $R_{\text{new}} = 0$. The dashed edges for the bottom graph can be removed, giving $R_{\text{new}} = \frac{3}{11}$.

B. Computing R_{new}

Although solving BTR exactly is an NP-hard problem, it has a rich combinatorial structure that allowed us to design an efficient approximation algorithm. The resulting algorithms were incorporated in our NET-SYNTHESIS software [15] (publicly available at www.cs.uic.edu/~dasgupta/network-synthesis/).

Although it is impossible to provide all details of the algorithmic approaches that was used for NET-SYNTHESIS, we provide some high-level details of the algorithm used; the reader can find further details, correctness proofs and algorithmic analysis in [14, 20]. It was proved in [20] that any strongly connected component (**SCC**) of the given graph $G = (V, E)$, say (V_1, E_1) with $V_1 \subseteq V$ and $E_1 = (V_1 \times V_1) \cap E$, can be classified as one of the two types: a *single parity SCC* if, for any two vertices $u, v \in V_1$, $u \xrightarrow{x} v$ exists in the **SCC** for exactly one x from $\{-1, 1\}$, and a *multiple parity SCC* if, for any two vertices $u, v \in V_1$, $u \xrightarrow{x} v$ exists in the **SCC** for both $x = 1$ and $x = -1$. A high-level view of the algorithmic approach is shown in Fig. 4.

The running time of NET-SYNTHESIS is dominated by Step 2. Theoretically, the worst-case running time of the algorithm is $O(n^3)$ when n is the number of vertices in G , but empirically the implementation allows us to calculate R_{new} for networks up to about five to

ten thousand nodes, thereby allowing us to compute the redundancy parameter for large networks. We expect that a future improved implementation of BTR will allow the calculation of redundancy values for even larger networks. Regarding optimality of the computed solution, theoretically NET-SYNTHESIS returns a solution that is a 3-approximation [14], *i.e.* $|E_{\text{solution}}|$ is no more than three times of that in an optimal solution in the worst case. However, extensive empirical evaluations reported in [14] suggest that in practice $|E_{\text{solution}}|$ is almost always close to optimal (within an extra 10% of the optimal).

C. Illustration of Redundancy Calculation for a Small Biological Networks

Our results of redundancy calculations on large-size biological and social networks are reported later, in Section VII, but here we illustrate the redundancy and minimal network calculations on a biological network that arises from the repetition of a fixed gene regulatory network over a number of cells. This gene regulatory network is formed among products of the segment polarity gene family, which plays an important role in the embryonic development of *Drosophila melanogaster*. The interactions incorporated in this network include translation (protein production from mRNA), transcriptional regulation, and protein-protein interactions. Two of the interactions are inter-cellular: specifically, the proteins wingless and hedgehog can leave the cell they are produced in and can interact with receptor proteins in the membrane of neighboring cells. We select this network for several reasons. First, the core part of the network for a single cell is small, consisting of 13 nodes and 22 edges, which enables analytical calculations of redundancy and visual depiction of redundant edges. Secondly, in spite of its simplicity and regularity, the associated multi-cell network does exhibit non-trivial redundancies due to the inter-cellular interactions and the cyclic arrangement of cells. The network for a single cell was first published in [21] and later in slightly modified form in [22, 23]. Fig. 5(a) shows the network of [21] with the interpretation of the regulatory role of PTC_m on the reaction $\text{CI} \rightarrow \text{CN}$ as $\text{PTC}_m \rightarrow \text{CN}$ and $\text{PTC}_m \dashv \text{CI}$. We note that the inter-cellular interactions are present at the whole cell membrane and not just the right boundary as shown for simplicity in all reconstructions. In a manner similar to that in other papers (*e.g.*, see [11]), we build a 1-dimensional multi-cellular version by considering a row of y cells, each of which has *separate* variables for each of the compounds, letting the cell-to-cell interactions be as in Fig. 5(a), but acting on both left and right neighbors, and using cyclic boundary conditions; see Fig. 5(b) for an illustration.

If the network contains $y > 2$ cells, then

- the number of vertices and edges are $13y$ and $22y$, respectively; and

1. Partition G into **SCCs**, say $C_1 = (V_1, E_1), C_2 = (V_2, E_2), \dots, C_p = (V_p, E_p)$
2. An **SCC** is a single parity component if, for every pair of nodes u and v , both $u \overset{-1}{\Rightarrow} v$ and $u \overset{1}{\Rightarrow} v$ do not exist in the **SCC**; otherwise it is a multiple parity component. Classify each **SCC** as single or multiple parity via a dynamic programming algorithm.
3. **for** each strongly connected component C_i **do**
 Use a heuristic to compute a solution, say E'_i , of BTR for C_i .
 The heuristic repeatedly selects an edge $u \overset{x}{\rightarrow} v$ that can be removed until no such edges exist in the **SCC**.
 Several criteria are used to select $u \overset{x}{\rightarrow} v$, such as:
 - parity of C_i (computed in Step 2)
 - length of the alternate path $u \overset{x}{\Rightarrow} v$
 - size (number of nodes) of C_i**endfor**
4. Build the following directed acyclic graph $G_S = (V_S, E_S)$ from G . At the end of the transformation, every edge e of G will be replaced by at most four edges in G_S ; we say that these (at most four) edges are “generated” by e . The proof of correctness of the algorithm shows that, for each edge e , all or none of the edges generated by e will be in the computed solution of G_S in Step 5.
 - for** $i = 1, 2, \dots, p$ **do**
 - if** C_i is of multiple parity **then**
 replace C_i by a node y_i
 if there is a directed edge (u, v) with $u \notin C_i$ and $v \in C_i$ **then** add the two edges $u \overset{-1}{\rightarrow} y_i$ and $u \overset{1}{\rightarrow} y_i$
 if there is a directed edge (u, v) with $u \in C_i$ and $v \notin C_i$ **then** add the two edges $y_i \overset{-1}{\rightarrow} v$ and $y_i \overset{1}{\rightarrow} v$
 - endif**
 - if** C_i is of single parity **then**
 pick any vertex $v \in C_i$; let $I^+ = \{x \in C_i \mid v \overset{1}{\Rightarrow} x \text{ exists in } C_i\}$, and $I^- = \{x \in C_i \mid v \overset{-1}{\Rightarrow} x \text{ exists in } C_i\}$
 replace C_i by four nodes $y_i^+, y_i^{++}, y_i^-, y_i^{--}$, and four edges $y_i^+ \overset{1}{\rightarrow} y_i^{++}, y_i^+ \overset{-1}{\rightarrow} y_i^{--}, y_i^- \overset{-1}{\rightarrow} y_i^{++}, y_i^- \overset{1}{\rightarrow} y_i^{--}$
 - for** every edge $u \overset{x}{\rightarrow} v$ with $u \notin C_i$ and $v \in C_i$ **do**
 if $v \in I^+$ **then** add the two edges $u \overset{x}{\rightarrow} y_i^+$ and $u \overset{-x}{\rightarrow} y_i^-$
 if $v \in I^-$ **then** add the two edges $u \overset{-x}{\rightarrow} y_i^+$ and $u \overset{x}{\rightarrow} y_i^-$
 endfor
 - for** every edge $u \overset{x}{\rightarrow} v$ with $u \in C_i$ and $v \notin C_i$ **do**
 if $v \in I^+$ **then** add the two edges $y_i^{++} \overset{x}{\rightarrow} v$ and $y_i^{--} \overset{-x}{\rightarrow} v$
 if $v \in I^-$ **then** add the two edges $y_i^{++} \overset{-x}{\rightarrow} v$ and $y_i^{--} \overset{x}{\rightarrow} v$
 endfor
 - endif**
 - endfor**
5. Solve BTR for G_S optimally by a greedy approach; let $E'_S \subseteq E_S$ be this solution.
6. Our solution E_{solution} of BTR for G is as follows:
 Include all the edges in $(\cup_{i=1}^p E'_i)$ in E_{solution}
for every edge e of G **do**
 if the set of edges generated by e is in E'_S **then** include e in E_{solution}
endfor

FIG. 4. A high-level view of the algorithmic approach in NET-SYNTHESIS to perform BTR.

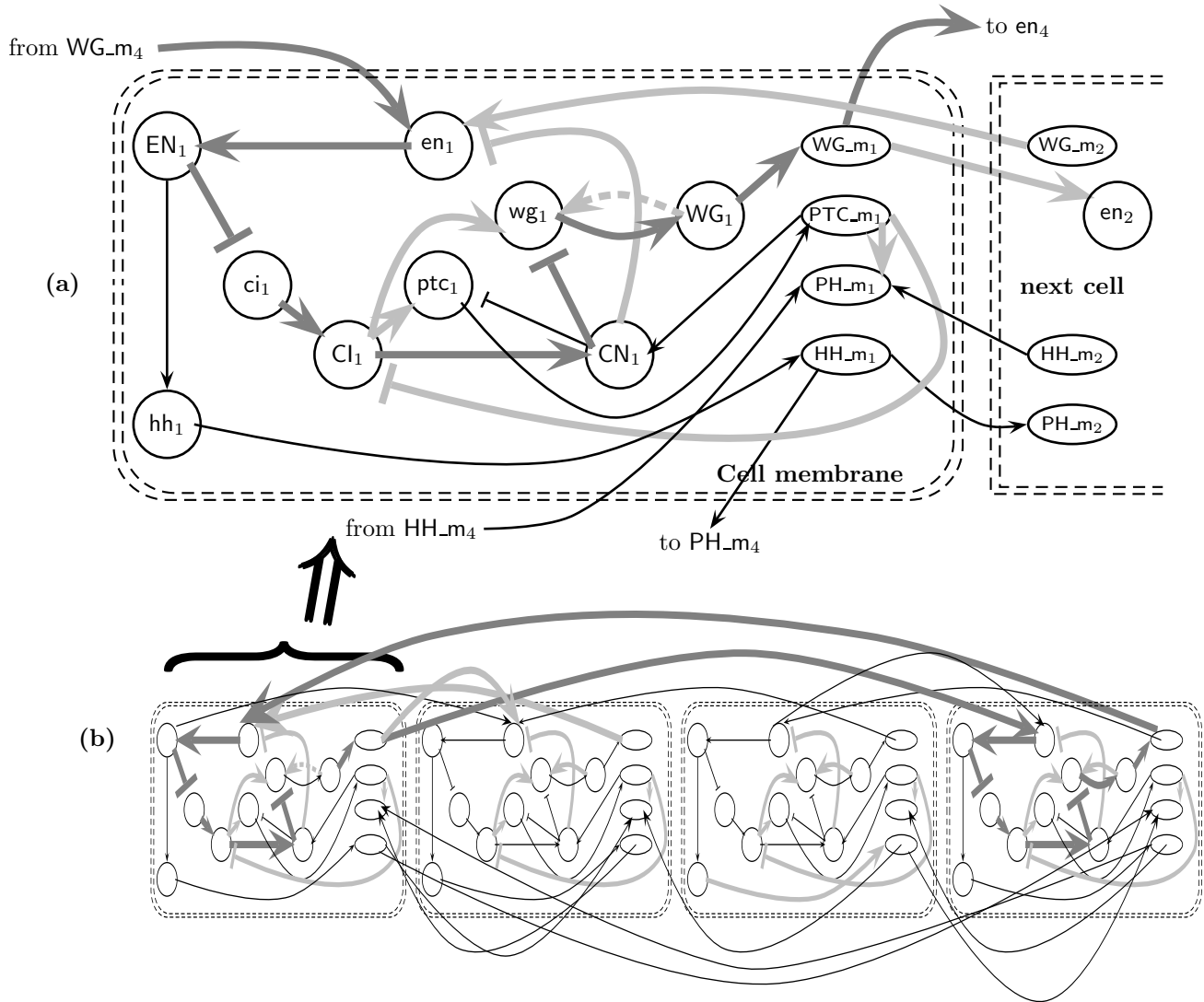


FIG. 5. (a) The *Drosophila* segment polarity network for a single cell, redrawn from [21]. (b) A network of 4 cells. The redundant edges in each cell are colored light gray. The dark gray edges form an alternate pathway of same parity for the edge $WG_1 \rightarrow wg_1$.

- NET-SYNTHESIS, after performing BTR, keeps $16y - 2$ edges, giving $R_{\text{new}} = \frac{6y+2}{22y} \approx \frac{3}{11}$.

Identifying a molecule in the i^{th} cell via a subscript i , NET-SYNTHESIS removed the following edges:

- the two edges $WG_{m_2} \rightarrow en_1$ and $WG_{m_1} \rightarrow en_2$, and
- the set of six edges from each cell i : $PTC_{m_i} \rightarrow PH_{m_i}$, $PTC_{m_i} \dashv Cl_i$, $WG_i \rightarrow wg_i$, $CN_i \dashv en_i$, $Cl_i \rightarrow wg_i$ and $Cl_i \rightarrow ptc_i$

As can be seen, the redundancies depend in a non-trivial manner on higher-order connections. For example, the

light gray edge $WG_1 \rightarrow wg_1$ is redundant because of the alternate dark gray pathway shown in Fig. 5.

D. Computing the Confidence Parameter for R_{new}

We apply our redundancy measure on seven biological networks and four social networks (see Table I). For each (social or biological) network G in Table I, except networks (9) and (10), having a redundancy value of $R_{\text{new}}(G)$, we generated 100 random networks, and computed the redundancies $R_{\text{new}}(G_{\text{random}_1})$, $R_{\text{new}}(G_{\text{random}_2})$, \dots , $R_{\text{new}}(G_{\text{random}_{100}})$ of these random

networks. We then use a (unpaired) one-sample student's t -test to determine the probability that $R_{\text{new}}(G)$ can be generated by a distribution that fits the data points $R_{\text{new}}(G_{\text{random}_1}), \dots, R_{\text{new}}(G_{\text{random}_{100}})$.

The current implementation of NET-SYNTHESIS runs slowly due to its intensive disk access on networks (9) and (10) in Table I because network (9) is very dense (an average degree of 9.62 on 1133 nodes) and network (10) has a very large number of edges (24316 edges). Redundancy analysis of a single random graph generated for either of these two networks requires a week or more, and any meaningful statistics would require on the order of 100 random graphs for each network. Due to the prohibitive time requirements we were not able to report p -values for these two networks. Since the characteristics of various biological and social networks are of different nature, we generate random networks for the various networks using two different methods as explained below.

Ideally, for networks of a particular type, one would prefer to use an accurate generative null model for highest accuracy in p -values. For signaling and transcriptional biological networks (networks (1)–(5) in Table I), reference [14], based on extensive literature review of similar kind of biological networks in prior papers, arrived at the characteristics of a generative null model that is described below and used by us for these networks³. One of the most frequently reported topological characteristics of such networks is the distribution of in-degrees and out-degrees of nodes, which exhibit a degree distribution that is close to a power-law or a mixture of a power law and an exponential distribution [25–27]. Specifically, transcriptional regulatory networks have been reported to exhibit a power-law out-degree distribution, while the in-degree distribution is more restricted [24, 28]. Based on such topological characterizations of signaling and transcriptional networks reported in the literature, [14] used the following degree distributions for the purpose of generating random networks for the biological transcriptional and signaling networks such as the ones in (1)–(5) in Table I:

- The number of vertices is the same as the network G whose redundancy value was computed.
- The in-degree and out-degree distributions of the random networks are as follows:
 - The distribution of in-degree of the networks is *exponential*, i.e., $\Pr[\text{in-degree}=x] = c_1 e^{-cx}$ with $\frac{1}{2} < c_1 < \frac{1}{3}$ and a maximum in-degree of 12.
 - The distribution of out-degree of the networks is governed by a *power-law*, i.e., for $x \geq 1$,

³ Our simulations with the alternate Markov-chain model used for the remaining networks show that the p -values still remain negligibly small; this is consistent with similar observations in another context made by Shen-Orr *et al.* [24].

$\Pr[\text{out-degree}=x] = c_2 x^{-c}$, for $x = 0$ $\Pr[\text{out-degree}=0] \geq c_2$ with $2 < c_2 < 3$ and a maximum out-degree of 200.

- The parameters in the above distribution are adjusted such that the sum of in-degrees of all vertices are equal to the sum of out-degrees of all vertices and the expected number of edges is the same as G .
- The percentage for activation/inhibition edges in the random network is the same as in G .

Each of the r random networks with these degree distributions are generated using our private implementation of the method suggested by Newman, Strogatz and Watts in [29].

For social networks, for the *C. elegans* metabolic network and for the oriented PPI network (networks (6)–(11) in Table I), in the absence of a consensus on an accurate generative null model, we generated the r random networks using a Markov-chain algorithm [30] in a similar manner as in, say [24], by starting with the real network G and repeatedly swapping randomly chosen pairs of connections in the following manner⁴:

repeat

choose two edges of $G = (V, E)$, $a \xrightarrow{x} b$ and $c \xrightarrow{y} d$,
randomly and uniformly ($x, y \in \{-1, 1\}$)

if $x \neq y$ or $a = c$ or $b = d$
or $a \xrightarrow{x} d \in E$ or $c \xrightarrow{y} b \in E$

then discard this pair of edges

else the random network contains the edges

$a \xrightarrow{x} d$ and $c \xrightarrow{y} b$ instead of $a \xrightarrow{x} b$ and $c \xrightarrow{y} d$

until 20% of edges of G has been swapped

V. MEASURE OF MONOTONICITY FOR BIOLOGICAL NETWORKS

To explain the intuition behind the computation of a monotonicity measure of the dynamics of a biological system, we start by relating the time-dynamics of the system with the graph-theoretic model of the network in the following way [10–12]. The time-varying system as defined by Equation (3) defines a labeled-graph model $G = (V, E, w)$ of the biological network in the following manner:

- $V = \{x_1, \dots, x_n\}$;
- if $\frac{\partial f_j}{\partial x_i} \geq 0$ for all $x(t) = (x_1(t), x_2(t), \dots, x_n(t))$ and $\frac{\partial f_j}{\partial x_i} > 0$ for some $x(t)$,
then $(x_i, x_j) \in E$ and $w(x_i, x_j) = 1$;

⁴ Shen-Orr *et al.* [24] considers swapping about 25% of the edges.

- if $\frac{\partial f_j}{\partial x_i} \leq 0$ for all $x(t)$ and $\frac{\partial f_j}{\partial x_i} < 0$ for some $x(t)$, then $(x_i, x_j) \in E$ and $w(x_i, x_j) = -1$.

(we assume that, for each i and j , either $\frac{\partial f_j}{\partial x_i} \geq 0$ for all x or $\frac{\partial f_j}{\partial x_i} \leq 0$ for all x .)

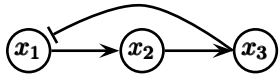


FIG. 6. Network for the system in Equation (5).

As an example, consider the following biological model of testosterone dynamics [31, 32]:

$$\begin{aligned} \frac{dx_1}{dt}(t) &= \frac{A}{K + x_3(t)} - b_1 x_1(t) \\ \frac{dx_2}{dt}(t) &= c_1 x_1(t) - b_2 x_2(t) \\ \frac{dx_3}{dt}(t) &= c_2 x_2(t) - b_3 x_3(t) \end{aligned} \quad (5)$$

The corresponding labeled network for this system is shown in Fig. 6. It is easy to show that (5) is *not* monotone with respect to \preceq_s , for all possible s . On the other hand, if we remove the term involving x_3 in the first equation, we obtain a system that is monotone with respect to \preceq_s , $s = (1, 1, 1)$. A cause of non-monotonicity of the system is the existence of *sign-inconsistent* paths between two nodes in an *undirected* version of the network, *i.e.*, the existence of both an activation and an inhibitory path between two nodes when *the directions of the edges are ignored*. To be precise, define a closed *undirected chain* in the labeled graph G as a sequence of vertices x_{i_1}, \dots, x_{i_r} such that $x_{i_1} = x_{i_r}$, and such that for every $\lambda = 1, \dots, r-1$ either $(x_{i_\lambda}, x_{i_{\lambda+1}}) \in E$ or $(x_{i_{\lambda+1}}, x_{i_\lambda}) \in E$. Then, the following result holds [11] (see also [33] and [34, page 101]).

Lemma 2 [11] *Consider a dynamical system (3) with associated directed labeled graph G . Then, (3) is monotone with respect to some orthant order if and only if all closed undirected chains of G have parity 1.*

Note that the combinatorial characterization of monotonicity in Lemma 2 is via the absence of *undirected* closed chains of parity 1. Thus, in particular, any monotone system has

- (a): no negative feedback loops, and
- (b): no incoherent feed-forward-loops.

However, some systems may not be monotone *even if* (a) and (b) hold; see Fig. 7 for an example.

Lemma 2 leads in a natural manner to the following *sign consistency* (SC) problem to determine how monotone a system is [11, 35].

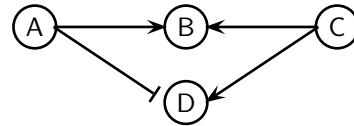


FIG. 7. A non-monotone system with no negative feedback loops and no incoherent feed-forward loops.

Problem name:: Sign Consistency (SC).

Instance:: a directed graph $G = (V, E)$ with an edge labeling function $w: E \mapsto \{-1, 1\}$.

Valid Solution:: a vertex labeling function $L: V \rightarrow \{-1, 1\}$.

Goal:: maximize $|F|$ where $F = \{(u, v) \mid w(u, v) = L(u)L(v)\}$ is a set of “consistent” edges.

Similar to our redundancy measure, we define the *degree of monotonicity* of a network to be

$$M = \frac{|F|}{|E|} \quad (6)$$

where F is the set of consistent edges in an optimal solution. The $|E|$ term in the denominator of the above definition translates to a min-max normalization of the measure, and ensures that $0 < M < 1$. Note that *the higher the value of M is the more monotone the network is* (cf. [11, 35]).

A. Computing M

In [11] a semidefinite-programming (SDP) based approximation algorithm is described for SC that has a worst-case theoretical guarantee of returning at least about 88% of the maximum number of edges. The algorithm was implemented in MATLAB (the MATLAB codes are publicly available at www.math.rutgers.edu/~sonntag/desz_README.html). Other algorithmic implementations of the SC problems are described in [35, 36].

B. Computing Correlation Between M and R_{new}

After obtaining the ordered pair of six values $(M_1, R_{\text{new}_1}), \dots, (M_6, R_{\text{new}_6})$ of M and R_{new} for the first six networks in Table I, we computed the standard Pearson product moment correlation coefficient $r = \frac{\sum_{i=1}^6 (R_{\text{new}_i} - \overline{R_{\text{new}}})(M_i - \overline{M})}{\sqrt{\sum_{i=1}^6 (R_{\text{new}_i} - \overline{R_{\text{new}}})^2 \sum_{i=1}^6 (M_i - \overline{M})^2}}$, where $\overline{R_{\text{new}}} = \frac{\sum_{i=1}^6 R_{\text{new}_i}}{6}$ and $\overline{M} = \frac{\sum_{i=1}^6 M_i}{6}$ are the average redundancy and monotonicity values, respectively. The possible values of r always lie in the range $[-1, 1]$, and values -1

and 1 signify strongest negative and positive correlations, respectively. A p -value for this correlation was calculated by a T-test with two-tailed distribution and unequal variance to show the probability of getting a correlation as large as the observed value by random chance when the true correlation is zero.

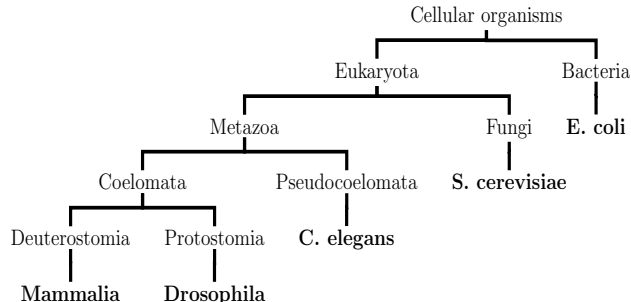


FIG. 8. An unweighted species tree of the organisms for our biological networks, constructed using the Taxonomy Browser resources of NCBI [37]. The tree is not drawn to scale.

VI. NETWORK DATA

We selected a total of 11 networks, seven biological ones and four social ones. We selected these networks with the following criteria in mind:

- The biological networks were selected with an eye towards covering a diverse set of species on the evolutionary scale and towards covering networks of diverse natures (*e.g.*, metabolic, transcriptional); a species tree of the biological organisms for our networks is shown in Fig. 8.
- The social networks were selected covering interactions in different social environments.
- The networks span a wide range on size (number of edges ranging from 135 to 24316) and density (average degree ranging from 1.3 to 13.4) to demonstrate that our new redundancy measure can be computed efficiently for a large class of networks.

Table I provides more details and sources for these networks.

VII. RESULTS AND DISCUSSIONS

In Table II we show the tabulation of redundancy and, when appropriate, also monotonicity values for our networks. Because of their large sizes, p -values for the redundancy measure could not be estimated very reliably for networks (9) and (10) since they require runs on many random networks, each of which would take upwards of a

week; thus we do not report p -values for these networks. The extremely low p -values in Table II indicate that the real networks' redundancy values cannot be generated by a distribution that fits the redundancies of the equivalent random graphs.

If one prefers, a normalization of the redundancy values of the networks for which randomly generated networks are available can be performed as follows. For each of the nine networks, we first computed the standardized redundancy value for each of the 100 random networks to eliminate sampling bias (for a sample x_1, x_2, \dots, x_m with average μ and standard deviation σ , the standardized value of x_i is given by $\frac{x_i - \mu}{\sigma}$). Then, we calculated the standardized range (difference between maximum and minimum) of these 100 standardized redundancy values. Finally, we normalized original redundancy value by dividing them by this standardized range. The resulting normalized values are shown in Table III (for comparison purposes, the normalized redundancy values are scaled so that their summation is exactly the same as the summation of original redundancy values). As can be seen, the ranks of both original and normalized values are almost the same (in the order (5), (1), (3), (11), (2), (4), (7), (6), (8) and (5), (1), (3), (11), (4), (2), (7), (6), (8), respectively) and the relative magnitudes of the values are similar whether one uses the normalized or original values, and thus all of our conclusions are valid in either case. Thus, in the rest of the paper, we use the original redundancy values with the understanding that all of our conclusions are valid for the normalized values as well.

In spite of our somewhat limited set of experiments, our results do point to some interesting hypotheses, which we summarize below.

A. R_{new} can be computed quickly for large networks and is statistically significant

As our simulations show, the new redundancy measure can be computed quickly for networks up to thousands of nodes; for example, typically NET-SYNTHESIS takes from a few seconds up to a minute for networks having up to 1000 nodes or edges. This is a desirable property of any redundancy measure so that it can be used by future researchers as biological and social networks grow in number and size. Moreover, the extremely low p -values suggests statistical significance of the new measure.

B. Redundancy variations in biological networks

We focus our attention to the variations of the redundancy values for the five transcriptional/signaling biological networks in our dataset and make the following observations.

a. Transcriptional vs. signaling networks Networks (1), (3) and (6) are transcriptional networks with all having similar low redundancies (0.062, 0.068 and 0.06).

TABLE I. Network data with sources. *If duplicated edges were present in the original network, they were removed in calculation of number of edges.*

	Number of nodes (n)	Number of edges (m)	Average degree (m/n)	Brief Description and Reference
Biological Networks				
(1)	311	451	1.45	<i>E. coli</i> transcriptional regulatory network constructed by Shen-Orr, Milo, Mangan and Alon in [24] for direct regulatory interactions between transcription factors and the genes or operons they regulate; see http://www.nature.com/ng/journal/v31/n1/full/ng881.html .
(2)	512	1047	2.04	<i>Mammalian</i> network of signaling pathways and cellular machines in the hippocampal CA1 neuron constructed by Ma'ayan <i>et al.</i> [38]; see http://www.sciencemag.org/content/309/5737/1078.abstract
(3)	418	544	1.3	<i>E. coli</i> transcriptional regulatory network (updated version of the network constructed by Shen-Orr, Milo, Mangan and Alon in [24]); see http://www.weizmann.ac.il/mcb/UriAlon/Papers/networkMotifs/colil1_1Inter_st.txt
(4)	59	135	2.28	<i>T cell large granular lymphocyte</i> (T-LGL) survival signaling network constructed by Zhang <i>et al.</i> [39]; see http://www.pnas.org/content/105/42/16308.abstract .
(5)	690	1082	1.56	<i>S. cerevisiae</i> transcriptional regulatory network constructed by Milo <i>et al.</i> [40] showing interactions between transcription factor proteins and genes; see http://www.sciencemag.org/cgi/content/abstract/298/5594/824 .
(6)	651	2040	3.13	<i>C. elegans</i> metabolic network constructed by Jeong <i>et al.</i> [41] and also used by Duch and Arenas in [42].
(7)	786	2453	3.12	An oriented version of an unweighted PPI network constructed from <i>S. cerevisiae</i> interactions in the BioGRID database by Gitter, Klein-Seetharaman, Gupta and Bar-Joseph [43].
Social Networks				
(8)	198	2742	13.84	Network of Jazz musicians [44].
(9)	1133	10903	9.62	List of edges of the network of e-mail interchanges between members of the University Rovira i Virgili (Tarragona) [45].
(10)	11240	24316	2.16	Network of users of the Pretty-Good-Privacy algorithm for secure information interchange; edges connect users that trust each other [46].
(11)	1169	1912	1.63	Enron email network; available from UC Berkeley Enron Email Analysis (http://bailando.sims.berkeley.edu/enron_email.html).

On the other hand, network (2) is a signaling network and network (4) is also *predominantly* signaling, though it includes four transcriptional edges; these two mammalian signal transduction networks have similar mid-range redundancies, namely 0.434 and 0.438, respectively. We hypothesize that in general transcriptional networks are less redundant than signaling networks. A straightforward supporting evidence for this is the higher average degree of signaling networks as compared to the transcriptional ones. Transcriptional networks have indeed been reported to have a feed-forward structure with few feedback loops and relatively low cross-talk [47], whereas [38] reports a large strongly connected component for their studied signaling networks (which makes it

possible to reach almost any node from any input node).

b. Role of currency metabolites in redundancy of metabolite networks Our data-source for the *C. elegans* metabolic network includes two types of nodes, the *metabolites* and *reaction* nodes, and the edges are directed either from those metabolites that are the reactants of a reaction to the reaction node, or from the reaction node to the products of the reaction. In this representation, redundant edges appear if both (one of) the reactant(s) and (one of) the product(s) of a reaction appear as reactants of a different reaction, or conversely, both (one of) the reactant(s) and (one of) the product(s) of a reaction appear as products of a different reaction. Because a reaction cannot go forward if one of its re-

TABLE II. (a) Topological redundancy and (b) monotonicity values. Higher values of R_{new} (respectively, M) imply more redundancy (respectively, monotonicity). In general, a p -value below 10^{-4} indicates statistical significance. N/A means not applicable; — indicates p -value could not be computed in reasonable time with the current implementation of NET-SYNTHESIS because of its extensive disk access for networks that are too large or dense. Note that the p -values depend not only on the average redundancies of the random networks but also on the higher order moments.

Network	(a)			(b)
	R_{new}	p -value	Redundancy average redundancy of random networks	Monotonicity M
Biological Networks				
(1) <i>E. Coli</i> transcriptional	0.062	1.43×10^{-29}	0.188	0.796
(2) <i>Mammalian</i> signaling	0.434	4.4×10^{-52}	0.576	0.593
(3) <i>E. Coli</i> transcriptional	0.068	2.61×10^{-9}	0.099	0.862
(4) T-LGL signaling	0.438	1.15×10^{-11}	0.350	0.867
(5) <i>S. cerevisiae</i> transcriptional	0.060	9.34×10^{-43}	0.228	0.926
(6) <i>C. elegans</i> metabolic	0.669	2.2×10^{-147}	0.790	0.444
(7) Oriented <i>S. cerevisiae</i> protein interactions	0.481	3.68×10^{-111}	0.593	N/A
Social Networks				
(8) Jazz musicians network	0.897	1.06×10^{-107}	0.929	N/A
(9) Email network at University Rovira i Virgili	0.840	—	—	N/A
(10) Secure information interchange user network	0.486	—	—	N/A
(11) Enron email network	0.352	2.14×10^{-68}	0.377	N/A

TABLE III. Normalization keeps relative magnitudes and ranks of values similar to that in the original.

	Networks									
	(1)	(2)	(3)	(4)	(5)	(6)	(7)	(8)	(11)	
Original Redundancy R_{new}	0.062	0.434	0.068	0.438	0.06	0.669	0.481	0.897	0.352	
Normalized Redundancy \widehat{R}_{new}	0.048	0.364	0.070	0.319	0.043	0.708	0.497	1.112	0.295	

actants is not present, the redundant edges are not biologically redundant and cannot be eliminated. Our result of a surprisingly high redundancy value for the metabolic network nevertheless indicates a high abundance of a pattern, which warrants further investigation.

One possibility we considered is that one of the reactions is essentially a *dimerization* of a compound and its slightly modified variant. However, we found no strong support for this case. Another possibility is that metabolites that participate in a large number of reactions will have a higher chance to be the reactant or product of such “redundant” edges. There is a biological basis for this possibility in the existence of *currency metabolites*. Currency metabolites (sometimes also referred to as *carrier* or *current* metabolites) are plentiful in normally functioning cells and occur in widely different exchange processes. For example, ATP can be seen as the energy currency of the cell. Because of their wide participation in diverse reactions, currency metabolites tend to be the highest

degree nodes of metabolic networks. There is some discussion in the literature on how large the group of currency metabolites is, but the consensus list includes H_2O , ATP, ADP, NAD and its variants, NH_4^+ , and PO_4^{3-} (phosphate) [48, 49].

Our data source for the *C. elegans* metabolic network indicates the identity of the 10 highest in-degree nodes (as a group) and the 10 highest out-degree nodes (as a group). Out of the 13 distinct nodes in the aggregate of these two groups, 11 belong in the consensus list of currency metabolites, leaving out co-enzyme A and L-glutamate. We found that when we rank the nodes of the network by the number of redundant edges (as found by NET-SYNTHESIS) incident upon them and consider the top 17 nodes in this rank order, they include all the 13 highest degree nodes in the original networks. Thus we can conclude that the topological redundancy of the *C. elegans* metabolic network is largely due to its inclusion of currency metabolites.

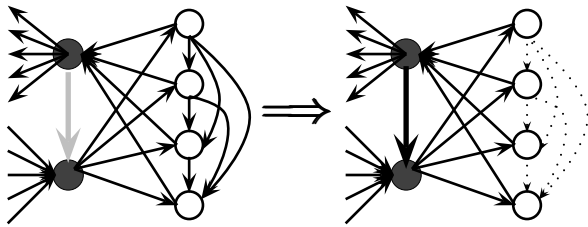


FIG. 9. Adding the edge colored light gray may increase the redundancy of the social network drastically (removed edges shown as dotted).

C. Redundancy of Social vs. Biological Networks

The results in Table II seem to suggest that social networks are more redundant than biological networks. In fact, the two most redundant networks in the table are the two social networks (8) and (9) which have redundancies about twice than that of any biological networks considered, and the remaining two social networks have redundancies comparable to the highest redundancy of the biological networks. We hypothesize that in general this is the case. This hypothesis is perhaps not very surprising in the context of past research as explained below.

The research work of Navlakha and Kingsford [50] suggests that biological networks may grow and evolve *quite differently* than social networks. In particular, they show that models for biological networks may perform poorly for social networks and vice versa. It is conceivable that different models may give rise to different magnitudes of redundancy.

Some previous research works (*e.g.*, see [51–53]) ascertain that social networks tend to exhibit *assortativity* (*i.e.*, highly connected nodes tend to be connected with other high degree nodes), whereas biological networks typically show *dissortativity* (*i.e.*, high degree nodes tend to attach to low degree nodes). It is not difficult to see that such properties may lead to the difference in redundancies for the two types of networks; For example, in Fig. 9 an edge between two nodes of high degree results in removal of a large number of edges. To check the general hypothesis of assortativity for our specific networks, we computed the assortativity coefficient for a network as defined in [52]. This coefficient is calculated in the following manner. First, we ignore the direction of edges obtaining an undirected graph $G = (V, E)$ from the given directed graph. Then, the assortativity coefficient r is computed by the following formula:

$$r = \frac{\frac{1}{|E|} \sum_{\{u,v\} \in E} d_u d_v - \left[\frac{1}{2|E|} \sum_{\{u,v\} \in E} (d_u + d_v) \right]^2}{\frac{1}{2|E|} \sum_{\{u,v\} \in E} [(d_u)^2 + (d_v)^2] - \left[\frac{1}{2|E|} \sum_{\{u,v\} \in E} (d_u + d_v) \right]^2}$$

where d_u denotes the degree of a node u . It is known that $-1 \leq r \leq 1$, and more negative (respectively, more positive) values of r indicating more disassortativity (respectively, more assortativity) of the given network. As

Table IV shows, all biological networks are disassortative, whereas all but one social network are assortative.

Finally, social networks that are related to human behavior are often expected to exhibit a high degree of transitivity [54–56]. For example, the classical work of Leinhardt [56] asserts that the structure of interpersonal relations in children’s groups will progress in consistent fashion from less to more transitive organization as the children become older. Transitivity in this type of behavioral context translates to coherent type 1 feed-forward loops (*i.e.*, feed-forward loops of the form $A \rightarrow B$, $B \rightarrow C$ and $A \rightarrow C$), each of which contains a redundant edge, and thus higher transitivity immediately implies higher redundancy in our context. To check how far this general hypothesis holds for our specific networks, we calculated the transitivity coefficient for our networks. The transitivity coefficient τ of a directed network [57] is given by $\frac{\mu_3}{\mu_2 + \mu_3}$ where μ_2 and μ_3 are the number of *ordered* triplets of vertices that has two and three edges among them, respectively. We used an obvious algorithm to calculate this value; τ could not be calculated within reasonable time for the social network (10) in Table I because of its large number of nodes and edges. As shown in Table IV, all the biological networks have small transitivity coefficients, and among the social networks, network (8) has a value of τ that is significantly more than any of the biological networks.

D. Redundancy, minimality and orienting PPI networks

Protein interaction networks represent *physical* interactions among proteins. While many protein interactions have an orientation, the current maps of protein-protein interaction (PPI) networks are often unoriented (undirected) in part due to the limitations of the current experimental technologies such as [58]. Thus, there is an obvious interest in trying to orient these networks by, say, combining causal information at the cellular level. Unfortunately, most versions of the orientation problem is theoretically NP-hard [59, 60], and thus heuristics for such orientations may either not lead to all pathways of interest or lead to extra spurious pathways that are not supported [43, 60].

Our calculation of redundancy values and minimal networks provides a way to gain insight into a predicted orientation of a PPI network and to determine whether the predicted oriented network has a level of redundancy similar to those in known biological networks. Obviously, the lower the value of R_{new} is, the more compact is the construction of the oriented network. However, one must also ensure that the minimal network also contains the right kind of pathways, *e.g.*, paths in the “gold standard”. To this effect, we describe the results of this approach via the NET-SYNTHESIS software on an oriented PPI network from [43].

We first briefly review the method by which the ori-

TABLE IV. Values of the assortativity coefficient r and the transitivity coefficient τ . Negative values of r indicate disassortativity whereas positive values of r indicate assortativity.

		Network Index										
		Biological					Social					
		(1)	(2)	(3)	(4)	(5)	(6)	(7)	(8)	(9)	(10)	(11)
$r =$		-0.149	-0.106	-0.204	-0.089	-0.398	-0.060	-0.1377	+0.02	+0.07	+0.239	-0.44
$\tau =$		0.037	0.010	0.007	0.043	0.005	0.047	0.017	0.255	0.058	—	0.013

ented PPI network used by us was generated. The starting point for the network consisted of all physical interactions among yeast proteins from version 2.0.51 of BioGRID [61]. Edge weights were assigned based on the type and quantity of experimental support for each interaction, and low-weight edges were removed from the network. The network was oriented so as to maximize the weighted number of length-bounded paths between predetermined sources and targets, which were taken from yeast MAPK signaling pathways. The final set of 2435 edges included all oriented edges that belonged to any path with 5 or fewer edges between a source and target and edge weights were dropped for subsequent analysis. The sources, targets, PPI filtering and orientation algorithm are described more fully in [43].

Now we discuss the paths in the non-redundant network (after reduction via NET-SYNTHESIS) that are present in the gold standard. Several of the short source-target paths in this network correspond to known yeast MAPK signaling pathways, specifically the pheromone response and filamentous growth pathways (www.genome.jp/kegg/pathway/sce/sce04011.html). Fig. 10 depicts the union of all linear paths in the non-redundant network that have multiple consecutive edges that match a gold standard path. The paths that matched a gold standard path are *highly similar*, and the common gold standard edges in these hits are $\text{Ste7} \rightarrow \text{Fus3}$, $\text{Fus3} \rightarrow \text{Dig1}$ and $\text{Dig1} \rightarrow \text{Ste12}$.

E. Correlation between redundancy and network dynamics

The Pearson correlation coefficient between M and R_{new} is about -0.8 with a p -value of 0.0066. Thus, monotonicity is negatively correlated to redundancy (*i.e.*, higher values of redundancy are expected to lead to lower values of monotonicity and vice versa).

As explained before, monotonicity is known to be negatively correlated to negative feedback loops [11, 62]. Negative feedback loops also tend to increase the redundancy of signal transduction networks; see Fig. 11 for an illustration. Indeed, strongly connected components with at least one negative feedback loop were called a multiple parity components in [20] and played a significant role in redundancy calculations.

Furthermore, recent results of Kwon and Cho [63] on

the correlation between topological properties and robustness of networks are also consistent with the negative correlation that we obtained. The authors of that paper considered a weighted network model in which the state of each node is a real number in the range $\{-1, 1\}$ and the positive and negative weights of the connections represent the strengths of the excitatory or inhibitory connections, respectively. A negative (respectively, positive) feedback loop is then defined to be a simple cycle with odd (respectively, even) number of negative weights in the cycle, and the degree of robustness of a network is then defined by selecting a group of nodes randomly, perturbing the values of their states, and measuring the extent of change of states of various nodes in the network by computing the ratio of state values converging to a same final state to which the original initial state converged (biologically, this concept of robustness means the extent of maintaining the original stable state against given perturbations). Based on extensive simulation results, the authors concluded that networks with fewer negative feedback loops are likely to be more robust in their sense. More robustness with respect to perturbations suggests less influence of one node on another, and consequently fewer alternate pathways of the *same nature* from a node to another, indicating less redundancy values, whereas fewer negative feedback loops correspond to higher degree of monotonicity. Thus, their observation is, at least on an intuitive level, consistent with our finding.

F. Significance of a minimal network

It is certainly an interesting question to ask if a topologically minimal network has similar dynamical or functional properties as the original network. Note that the question does not make sense for the four (static) social networks (networks (8), (9), (10) and (11) in Table I), since the individual nodes in these networks usually do not have well-defined functions or dynamics, and one of their *most interesting* properties, namely connectivity, is *preserved* in the minimal network. The redundancy issue of the metabolic network (network (6) of Table I) is explained separately in detail in Section VII B 0 b. There is no associated dynamics with the oriented PPI network (network (7) of Table I). Thus, this question *only applies* for the first five biological networks (networks (1), (2), (3), (4) and (5)) in Table I. A dynamic descrip-

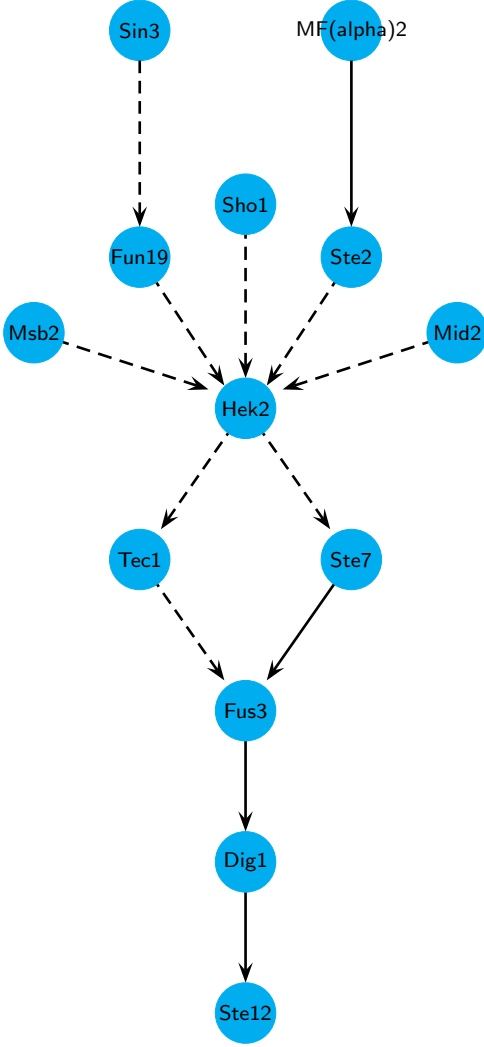


FIG. 10. (color online) Paths in the non-redundant oriented PPI network that match known yeast signaling pathways. Solid edges are present in the gold standard and dashed edges represent novel predictions.

tion/model of these networks would characterize dynamic behaviors, such as stability and response to external inputs. When the network has designated outputs or readouts, such as gene expression rates in transcriptional networks, it may be of interest to characterize the behavior of these outputs as a function of the inputs.

A topologically minimal network has the same input-output connectivity (reachability) as the original and thus the excitory or inhibitory influence between each input-output pair *is* preserved. It is minimal in the “information theoretic” sense in that any network with the same output behavior must be of at least this size. A correlation of the redundancy measure with the monotonicity of dynamics is explored in Section VII E. Will a topologically minimal network also have the same out-

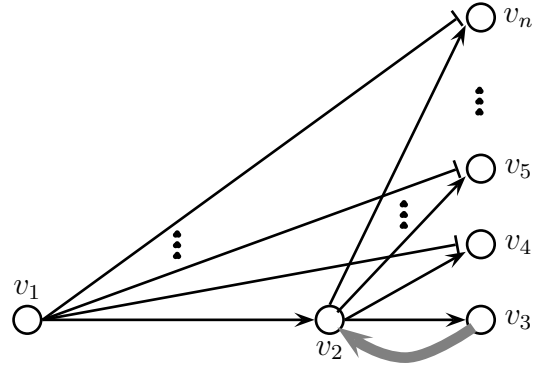


FIG. 11. The network shown has no negative feedback loops and no redundant edges. However, if we replace the gray activation edge $v_3 \rightarrow v_2$ to an inhibition edge $v_3 \dashv v_2$, a negative feedback loop is created and this makes all the remaining inhibitory edges in the network redundant (e.g., the edge $v_1 \dashv v_4$ is redundant because of the path $v_1 \rightarrow v_2 \rightarrow v_3 \dashv v_2 \rightarrow v_4$).

put behavior as the original one for the same input? In general, there is no such guarantee since the dynamics depend on what type of functions (“gate”) are used to combine incoming connections to nodes and the “time delay” in the signal propagation, both of which are omitted in the graph-theoretic representation of regulatory and signal-transduction networks such as (1)–(5) in Table I. For example, consider the two networks shown in Fig. 12 in which network (b) has a redundant connection $A \rightarrow C$. The functions of these two circuits could be different, however, depending on the “gate” function used to combine the inputs $B \rightarrow C$ and $A \rightarrow C$ in network (b). Due to the shared $A \rightarrow B \rightarrow C$ connectivity in the two networks, in both cases node C will be activated if A is *continuously supplied*. However, while network (a) merely implements a delay between C and A , the coherent type-1 feedforward loop indicated in (b) is what [64] calls a “sign-sensitive delay element” that filters spikes in signals (low-pass filter) *provided* that an “AND” gate combines the inputs to node C ; one example of such a circuit is that of the Arabinose system in *E.coli* [65]. In summary, deleting edges may result in functionalities that are not exactly the same.

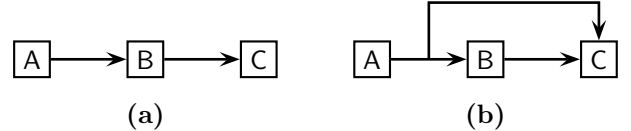


FIG. 12. Equivalence of dynamics depends on node functions.

However, despite the fact that a minimal network may not preserve *all* dynamic properties of the original one, a significant application of finding minimal networks lies

precisely in allowing one to identify redundant connections (edges). In this manner, one may focus on investigating the functionalities of these redundant edges, *e.g.*, identifying the manner in which their effect is cumulated with those of the other regulators of their target nodes could be a key step toward understanding the behavior of the entire network.

Thus, the tools developed here are of general interest as they not only provide a quantified measure of overall redundancy of the network, but also allow their identification of redundancies and hence help direct future research toward the understanding of the functional significance of the added links.

VIII. AVAILABILITY OF DATA AND SOFTWARE

Most of the data for the original network as well as those for the random networks used in the calculation of p -values for R_{new} are available from our website www.cs.uic.edu/~dasgupta/network-data/. The NET-SYNTHESIS software for calculating redundancies is available from our website www.cs.uic.edu/~dasgupta/network-synthesis/. MATLAB codes for computing monotonicity values are available from our website www.math.rutgers.edu/~sonntag/desz_README.html.

IX. CONCLUSIONS

In this paper we have defined a new combinatorial measure of redundancy of biological and social networks, and have illustrated its efficient computation on several small and large networks. We also noted some interesting hypotheses that one could draw from these results such as:

- Transcriptional networks are likely to be less redundant than signaling networks.
- The topological redundancy of the *C. elegans* metabolic network is largely due to its inclusion of currency metabolites.
- Social networks are prone to be more redundant than biological networks.
- Our calculation of redundancy values and minimal networks provides a way to gain insight into a predicted orientation of a protein-protein-interaction (PPI) network and determine whether the predicted oriented network has a level of redundancy similar to those in known biological networks.
- Our topology-based redundancy measure for biological signaling networks is statistically correlated with some measure of the dynamics of the network, namely higher redundancy is correlated to lower monotonicity and vice versa.

We believe that our fast and accurate computation of redundancy measure will help future researchers to further fine tune the measure and test it on a large-scale basis. An interesting question that has been partially addressed in the past literature but deserves further investigation is to determine the reasons of redundancy of various kinds of biological networks.

ACKNOWLEDGMENTS

We thank Sema Kachalo for the implementation of NET-SYNTHESIS and an implementation of the random graph generation method of Newman, Strogatz and Watts [29]. Réka Albert was partially supported by NSF grant CCF-0643529 and Eduardo Sontag was supported by NIH grant 1R01GM086881 during this work.

-
- [1] R. Kafri, A. Bar-Even and Y. Pilpel. *Transcription control reprogramming in genetic backup circuits*, Nature Genetics, 37, 295-299, 2005.
 - [2] B. Kolb and I. Q. Whishaw. *Fundamentals of Human Neuropsychology*, Freeman, New York, 1996.
 - [3] G. Tononi, O. Sporns and G. M. Edelman. *Measures of degeneracy and redundancy in biological networks*, Proc. Natl. Acad. Sci. USA, 96, 3257-3262, 1999.
 - [4] J. A. Papin and B. O. Palsson. *Topological analysis of mass-balanced signaling networks: a framework to obtain network properties including crosstalk*, Journal of Theoretical Biology, 227 (2), 283-297, 2004.
 - [5] N. Beckage, L. Smith, and T. Hills. *Semantic network connectivity is related to vocabulary growth rate in children*, The Annual Meeting of The Cognitive Science Society (CogSci), 2769-2774, 2010.
 - [6] L. DallAsta, I. Alvarez-Hamelin, A. Barrata, A. Vázquez and A. Vespignania. *Exploring networks with traceroute-like probes: Theory and simulations*, Theoretical Computer Science, 355, 6-24, 2006.
 - [7] G. Tononi, O. Sporns and G. M. Edelman. *A measure for brain complexity: relating functional segregation and integration in the nervous system*, Proc. Natl. Acad. Sci. USA, 91 (11), 5033-5037, 1994.
 - [8] G. Tononi, O. Sporns and G. M. Edelman. *A complexity measure for selective matching of signals by the brain*, Proc. Natl. Acad. Sci. USA, 93, 3422-3427, 1996.
 - [9] M. Hirsch. *Differential equations and convergence almost everywhere in strongly monotone flows*, Contemporary Mathematics, 17, 267-285, 1983.
 - [10] H. L. Smith. *Monotone Dynamical Systems*, Providence, R.I., AMS 1995.
 - [11] B. DasGupta, G. Andres Enciso, E. Sontag and Y. Zhang. *Algorithmic and complexity results for decompositions of biological networks into monotone subsystems*, Biosystems, 90 (1), 161-178, 2007.

- [12] D. Angeli and E.D. Sontag. *Monotone control systems*, IEEE Transactions on Automatic Control, 48, 1684-1698, 2003.
- [13] J. Monod and F. Jacob. *General conclusions: telenomic mechanisms in cellular metabolism, growth, and differentiation*, Cold Spring Harbor Symposium on Quantitative Biology, 26, 389-401, 1961.
- [14] R. Albert, B. DasGupta, R. Dondi, S. Kachalo, E. Sontag, A. Zelikovsky and K. Westbrook. *A novel method for signal transduction network inference from indirect experimental evidence*, Journal of Computational Biology, 14 (7), 927-949, 2007.
- [15] S. Kachalo, R. Zhang, E. Sontag, R. Albert and B. DasGupta. *NET-SYNTHESIS: A software for synthesis, inference and simplification of signal transduction networks*, Bioinformatics, 24 (2), 293-295, 2008.
- [16] S. Khuller, B. Raghavachari and N. Young. *On strongly connected digraphs with bounded cycle length*, Discrete Applied Mathematics, 69 (3), 281-289, 1996.
- [17] A. Wagner. *Estimating coarse gene network structure from large-scale gene perturbation data*, Genome Research, 12, 309-315, 2002.
- [18] V. Dubois and C. Bothorel. *Transitive reduction for social network analysis and visualization*, IEEE/WIC/ACM International Conference on Web Intelligence, 128-131, 2005.
- [19] J. Hann and M. Kamber. *Data Mining: Concepts and Techniques*, Morgan Kaufman Publishers, 2000.
- [20] R. Albert, B. DasGupta, R. Dondi and E. Sontag. *Inferring (biological) signal transduction networks via transitive reductions of directed graphs*, Algorithmica, 51 (2), 129-159, 2008.
- [21] G. von Dassow, E. Meir, E.M. Munro, and G.M. Odell. *The segment polarity network is a robust developmental module*, Nature, 406, 188-192, 2000.
- [22] R. Albert and H. G. Othmer. *The topology of the regulatory interactions predicts the expression pattern of the Drosophila segment polarity genes*, Journal of Theoretical Biology, 223, 1-18, 2003.
- [23] N. T. Ingolia. *Topology and robustness in the Drosophila segment polarity network*, PLoS Biology, 2(6), e123, 2004.
- [24] S. S. Shen-Orr, R. Milo, S. Mangan and U. Alon. *Network motifs in the transcriptional regulation network of Escherichia coli*, Nature Genetics, 31, 64-68, 2002.
- [25] R. Albert and A.-L. Barabási. *Statistical mechanics of complex networks*, Reviews of Modern Physics, 74 (1), 47-97, 2002.
- [26] L. Giot, J. S. Bader et al. *A protein interaction map of Drosophila melanogaster*, Science, 302, 1727-1736, 2003.
- [27] S. Li, C. M. Armstrong et al. *A map of the interactome network of the metazoan C. elegans*, Science, 303, 540-543, 2004.
- [28] T. I. Lee, N. J. Rinaldi et al. *Transcriptional regulatory networks in Saccharomyces cerevisiae*, Science, 298, 799-804, 2002.
- [29] M. E. J. Newman, S. H. Strogatz and D. J. Watts. *Random graphs with arbitrary degree distributions and their applications*, Physical Review E, 64 (2), 026118-026134, 2001.
- [30] R. Kannan, P. Tetali and S. Vempala. *Markov-chain algorithms for generating bipartite graphs and tournaments*, Random Structures and Algorithms, 14, 293-308, 1999.
- [31] J.D. Murray. *Mathematical Biology, I: An introduction*, New York, Springer, 2002.
- [32] G. Enciso and E. Sontag. *On the stability of a model of testosterone dynamics*, Journal of Mathematical Biology, 49, 627-634, 2004.
- [33] D. L. DeAngelis, W. M. Post and C. C. Travis. *Positive Feedback in Natural Systems*, Springer-Verlag, New York, 1986.
- [34] H. L. Smith. *Systems of ordinary differential equations which generate an order-preserving flow: A survey of results*, SIAM Reviews, 30, 87-111, 1988.
- [35] F. Hüffner, N. Betzler and R. Niedermeier. *Optimal edge deletions for signed graph balancing*, Workshop on Experimental Algorithms, Lecture Notes in Computer Science, 4525, 297-310, Springer-Verlag, 2007.
- [36] G. Gutin, D. Karapetyan and I. Razgon. *Fixed-Parameter Algorithms in Analysis of Heuristics for Extracting Networks in Linear Programs*, 4th International Workshop on Parameterized and Exact Computation, Lecture Notes in Computer Science, 5917, 222-233, Springer-Verlag, 2009.
- [37] ncbi.nlm.nih.gov/Taxonomy/CommonTree/wwwcmt.cgi.
- [38] A. Ma'ayan, S. L. Jenkins, S. Neves, A. Hasseldine, E. Grace, B. Dubin-Thaler, N. J. Eungdamrong, G. Weng, P. T. Ram, J. Jeremy Rice, A. Kershenbaum, G. A. Stolovitzky, R. D. Blitzer and R. Iyengar. *Formation of regulatory patterns during signal propagation in a mammalian cellular network*, Science, 309 (5737), 1078-1083, 2005.
- [39] R. Zhang, M. V. Shah, J. Yang, S. B. Nyland, X. Liu, J. K. Yun, R. Albert and T. P. Loughran. *Network model of survival signaling in large granular lymphocyte leukemia*, Proc. Natl. Acad. Sci. USA, 105 (42), 16308-16313, 2008.
- [40] R. Milo, S. Shen-Orr, S. Itzkovitz, N. Kashtan and D. U. Alon. *Network motifs: simple building blocks of complex networks*, Science, 298, 824-827, 2002.
- [41] H. Jeong, B. Tombor, R. Albert, Z. N. Oltvai and A.-L. Barabasi. *The large-scale organization of metabolic networks*, Nature, 407, 651-654, 2000.
- [42] J. Duch and A. Arenas. *Community identification using extremal optimization*, Physical Review E, 72, 027104, 2005.
- [43] A. Gitter, J. Klein-Seetharaman, A. Gupta and Z. Bar-Joseph. *Discovering pathways by orienting edges in protein interaction networks*, Nucleic Acids Research, 39 (4), e22, 2011.
- [44] P. Gleiser and L. Danon. *Community structure in jazz*, Advances in Complex Systems, 6, 565-573, 2003.
- [45] R. Guimera, L. Danon, A. Diaz-Guilera, F. Giralt and A. Arenas. *Self-similar community structure in a network of human interactions*, Physical Review E, 68, 065103, 2003.
- [46] M. Boguña, R. Pastor-Satorras, A. Diaz-Guilera and A. Arenas. *Models of social networks based on social distance attachment*, Physical Review E, 70, 056122, 2004.
- [47] G. Balázs, A.-L. Barabási and Z. N. Oltvai. *Topological units of environmental signal processing in the transcriptional regulatory network of Escherichia coli*, Proc. Natl. Acad. Sci. USA, 102, 7841-7846, 2005.
- [48] A. Wagner and D. A. Fell. *The small world inside large metabolic networks*, Proc. R. Soc. London, B, 268, 1803-1810, 2001.
- [49] P. Gerlee, L. Lizana and K. Sneppen. *Pathway identification by network pruning in the metabolic network of Escherichia coli*, Bioinformatics, 25 (24), 2009.
- [50] S. Navlakha and C. Kingsford. *Network archaeology: uncovering ancient networks from present-day interactions*,

- to appear in PLoS Computational Biology, 2011.
- [51] M. E. J. Newman. *Mixing patterns in networks*, Physical Review E, 67, 026126, 2003.
- [52] M. E. J. Newman. *Assortative mixing in networks*, Physical Review Letters, 89, 208701, 2002.
- [53] P.-S. Romualdo, A. Vázquez, and A. Vespignani. *Dynamical and Correlation Properties of the Internet*, Physical Review Letters, 87 (25), 2001.
- [54] P. W. Holland and S. Leinhardt. *Transitivity in structural models of small groups*, Comparative Group Studies, 2, 107-124, 1998.
- [55] C. Kemp and J. B. Tenenbaum. *The discovery of structural form*, Proc. Natl. Acad. Sci. USA, 105 (31), 10687-10692, 2008.
- [56] S. Leinhardt. *The development of transitive structure in children's interpersonal relations*, Behavioral Science, 18, 260-271, 1973.
- [57] S. Wasserman and K. Faust, *Social Network Analysis: Methods and Applications*, Cambridge University Press, 1994.
- [58] S. Fields. *High-throughput two-hybrid analysis: the promise and the peril*, FEBS Journal, 272 (21), 5391-5399, 2005.
- [59] E. M. Arkin and R. Hassin. *A note on orientations of mixed graphs*, Discrete Applied Mathematics, 116 (3), 271-278, 2002.
- [60] A. Medvedovsky, V. Bafna, U. Zwick and R. Sharan. *An algorithm for orienting graphs based on cause-effect pairs and its applications to orienting protein networks*, Algorithms in Bioinformatics, Lecture Notes in Computer Science, 5251, 222-232, Springer-Verlag, 2008.
- [61] C. Stark, B. Breitkreutz, T. Reguly, L. Boucher, A. Breitkreutz and M. Tyers. *BioGRID: a general repository for interaction datasets*, Nucleic Acids Research, 34, 535-539, 2006.
- [62] G. A. Enciso, H. L. Smith, and E. D. Sontag. *Non-monotone systems decomposable into monotone systems with negative feedback*, Journal of Differential Equations, 224, 205-227, 2006.
- [63] Y.-K. Kwon and K.-H. Cho. *Quantitative analysis of robustness and fragility in biological networks based on feedback dynamics*, Bioinformatics, 24 (7), 987-994, 2008.
- [64] U. Alon. *An Introduction to Systems Biology: Design Principles of Biological Circuits*, Chapman & Hall, 2006.
- [65] S. Mangan, A. Zaslaver and U. Alon. *The coherent feed-forward loop serves as a sign-sensitive delay element in transcription networks*, Journal of Molecular Biology, 334 (2), 197-204, 2003.